



# Nitrogen removal from natural gas using solid boron: A first-principles computational study

Qiao Sun <sup>a,\*</sup>, Meng Wang <sup>b</sup>, Zhen Li <sup>c,\*</sup>, Ping Li <sup>d</sup>, Weihua Wang <sup>d</sup>, Xiaojun Tan <sup>e</sup>, Aijun Du <sup>f,\*</sup>

<sup>a</sup> Centre for Theoretical Computational Molecular Science, Australian Institute for Bioengineering and Nanotechnology, The University of Queensland, QLD 4072, Brisbane, Australia

<sup>b</sup> Center for Bioengineering and Biotechnology, China University of Petroleum (East China), Qingdao 266555, China

<sup>c</sup> Institute of Superconducting & Electronic Materials, The University of Wollongong, NSW 2500, Australia

<sup>d</sup> School of Chemistry and Chemical Engineering, Qufu Normal University, Qufu, Shandong 273165, China

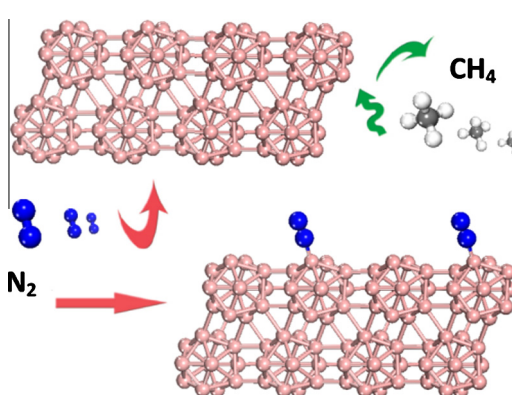
<sup>e</sup> College of Medical and Life Science, University of Jinan, Jinan, Shandong 250022, China

<sup>f</sup> School of Chemistry, Physics and Mechanical Engineering, Queensland University of Technology, Brisbane, QLD 4001, Australia

## HIGHLIGHTS

- CH<sub>4</sub> molecules can only form weak interactions with B<sub>12</sub> cluster, α-B<sub>12</sub> and γ-B<sub>28</sub> surfaces.
- N<sub>2</sub> forms relative strong interaction with these boron adsorbents.
- These boron adsorbents have very high selectiveness to capture N<sub>2</sub> from natural gas.
- The boron adsorbents can be promising materials for natural gas purification.

## GRAPHICAL ABSTRACT



## ARTICLE INFO

### Article history:

Received 3 December 2012

Received in revised form 14 March 2013

Accepted 15 March 2013

Available online 1 April 2013

### Keywords:

N<sub>2</sub>/CH<sub>4</sub> separation

Gas purification

DFT calculations

## ABSTRACT

Selective separation of nitrogen (N<sub>2</sub>) from methane (CH<sub>4</sub>) is highly significant in natural gas purification, and it is very challenging to achieve this because of their nearly identical size (the molecular diameters of N<sub>2</sub> and CH<sub>4</sub> are 3.64 Å and 3.80 Å, respectively). Here we theoretically study the adsorption of N<sub>2</sub> and CH<sub>4</sub> on B<sub>12</sub> cluster and solid boron surfaces α-B<sub>12</sub> and γ-B<sub>28</sub>. Our results show that these electron-deficiency boron materials have higher selectivity in adsorbing and capturing N<sub>2</sub> than CH<sub>4</sub>, which provides very useful information for experimentally exploiting boron materials for natural gas purification.

© 2013 Elsevier Ltd. All rights reserved.

## 1. Introduction

The demand for natural gas is expected to increase continuously in the coming years, because natural gas produces lower CO<sub>2</sub> emission than other fossil fuels. Novel transport technologies, the

remarkable reserves found, the lower overall costs and the environmental sustainability all point to natural gas as the primary energy source in the near future [1,2]. In fact, the demand for natural gas may exceed coal by 2020, due to its less pollution and higher use efficiency [3]. The natural gas reservoirs are usually far from final markets, and as a consequence it has to be transported either by pipelines as a gaseous mixture containing at least 75% of methane, or by tankers as liquefied natural gas containing at least 85% of methane [4]. The choice between the two transportation

\* Corresponding authors. Tel.: +61 7 33463996; fax: +61 7 33463992 (Q. Sun).

E-mail addresses: [q.sun@uq.edu.au](mailto:q.sun@uq.edu.au) (Q. Sun), [zhenl@uow.edu.au](mailto:zhenl@uow.edu.au) (Z. Li), [aijun.du@qut.edu.au](mailto:aijun.du@qut.edu.au) (A. Du).

technologies depends mainly on the distance and the volume of gas to be transferred.

Nitrogen is a common contaminant in natural gas and is quite difficult to be removed. It lowers the value of the natural gas and makes it untransportable to most pipelines. Natural gas can be accepted for pipeline transport-only it contains less amount of nitrogen, typically between 4% and 6%. Therefore several approaches (e.g. cryogenic separation, solid adsorption and membrane separation) have been developed for removing nitrogen. Cryogenic nitrogen removal is complex and expensive, prohibiting large-scale purification of natural gas [5]. Solid adsorption has been proposed as attractive alternatives for natural gas purification. However, most sorbents show weak interactions with methane and nitrogen, and unable to effectively separate them [3]. Conventional membrane technology cannot effectively separate nitrogen from natural gas because of the similar molecules kinetic diameters of methane and nitrogen ( $\sigma_{N_2} = 3.64 \text{ \AA}$ ,  $\sigma_{CH_4} = 3.80 \text{ \AA}$ ) [6]. Thus, very few materials are able to selectively adsorb nitrogen from natural gas, and it is highly significant to seek new materials with high selectivity and low cost for separation of nitrogen from natural gas.

In recent years, novel boron clusters and boron crystals have attracted extensive attentions [7–15], due to their unique physicochemical properties [12,16–19]. There are growing interests in exploring the structures and properties of pure boron clusters and boron containing compounds because they have a wide variety of applications from nuclear reactors to superhard, thermoelectric and high energy materials. In the recent article “Boron Cluster Come of Age”, Grimes commented the variety of boron clusters, such as neutral boranes, polyhedral boranes, and their derivatives, motivating us to reconsider the concept of covalent chemical bonding [20]. Among boron clusters,  $B_{12}$  icosahedron is the basic structural unit for the elementary boron solids (e.g. the well-known  $\alpha$ - $B_{12}$  and  $\gamma$ - $B_{28}$  crystals) although the  $B_{12}$  icosahedron is not stable when it is treated as a single isolated cluster [21–24]. Recently, boron-rich ternary compounds containing  $B_{12}$  icosahedra have attracted considerable attention since they exhibit important features on both fundamental and practical perspectives [7,9,12,25–27].

For crystal boron, the central unit (i.e.  $B_{12}$  icosahedron) of their structures is same to that of many boron rich compounds, and can be flexibly linked, joined, or fused into rigid framework structures [12,16–18,21,25,26,28–31]. The formation of  $B_{12}$  unit and its versatile connectivity are attributed to the “electron deficiency”, or hypovalency of boron. There are only four crystal phases reported for pure elementary boron: rhombohedral  $\alpha$ - $B_{12}$  [17,26,31] and  $\beta$ - $B_{106}$  [16] (with 12 and 106 atoms in the unit cell, respectively), tetragonal T-192 [18] (with 190–192 atoms per unit cell) and  $\gamma$ - $B_{28}$  (with 28 atoms in the unit cell).  $\alpha$ - $B_{12}$  consists of one  $B_{12}$  icosahedron per unit cell while  $\gamma$ - $B_{28}$  consists of icosahedral  $B_{12}$  clusters and  $B_2$  pairs in a NaCl-type arrangement [12]. Moreover, the electronic properties of the  $B_2$  pairs and  $B_{12}$  clusters in  $\gamma$ - $B_{28}$  are different, resulting in the charge transfer between  $B_{12}$  clusters and  $B_2$  pairs [12]. In this paper, we investigate the adsorption of  $N_2$  and  $CH_4$  on boron  $B_{12}$  icosahedron cluster and boron solid surfaces of  $\alpha$ - $B_{12}$  and  $\gamma$ - $B_{28}$ . The primary motivation is to identify solid boron crystals as new sorbents for natural gas purification.

## 2. Computational methods

The first-principles density-functional theory [32,33] with long range dispersion correction [34] (DFT-D) calculations were carried out using DMol3 module in Materials Studio [35,36]. The boron cluster and boron solid surfaces were fully optimized in the given symmetry using generalized gradient approximation treated by Perdew–Burke–Ernzerhof exchange–correlation potential. An all

electron double numerical atomic orbital augmented by  $d$ -polarization functions (DNP) was used as basis set. The self-consistent field (SCF) procedure was used with a convergence threshold of  $10^{-6}$  a.u. on energy and electron density. The direct inversion of the iterative subspace technique developed by Pulay was used with a subspace size 6 to speed up SCF convergence on these large clusters [37]. In order to achieve the SCF convergence when the gap between the highest occupied molecular orbital and the lowest unoccupied molecular orbital (HOMO–LUMO) is small, thermal smearing using finite-temperature Fermi function of 0.005 a.u. was used. Geometry optimizations were performed with a convergence threshold of 0.002 a.u./ $\text{\AA}$  on the gradient, 0.005  $\text{\AA}$  on displacements, and  $10^{-5}$  a.u. on the energy. The real-space global cutoff radius was set to be 4.10  $\text{\AA}$ . For the  $B_{12}$  cluster, the cluster was placed in a sufficiently large supercell ( $20 \text{ \AA} \times 20 \text{ \AA} \times 20 \text{ \AA}$ ) to avoid interactions with its periodic images. The cell parameters for  $\alpha$ - $B_{12}$  and  $\gamma$ - $B_{28}$  used for the calculations are all optimized. The optimized cell parameters of  $\alpha$ - $B_{12}$  and  $\gamma$ - $B_{28}$  are in good agreement with experimental measurements. In details, the optimized cell parameters of  $\alpha$ - $B_{12}$  are with the values of  $a = b = c = 5.052 \text{ \AA}$ ,  $\alpha = \beta = \gamma = 57.76^\circ$ , which are very close to the values of experimental measurement of  $a = b = c = 5.064 \text{ \AA}$ ,  $\alpha = \beta = \gamma = 58.10^\circ$  [38]. For  $\gamma$ - $B_{28}$ , the optimized cell parameters are  $a = 5.042 \text{ \AA}$ ,  $b = 5.598 \text{ \AA}$ ,  $c = 6.914 \text{ \AA}$ ,  $\alpha = \beta = \gamma = 90.0^\circ$ , which are also consistent with the experimental values of  $a = 5.054 \text{ \AA}$ ,  $b = 5.612 \text{ \AA}$ ,  $c = 6.987 \text{ \AA}$ ,  $\alpha = \beta = \gamma = 90.0^\circ$  [12]. The  $4 \times 4$   $\alpha$ -boron (001) and  $2 \times 2$   $\gamma$ -boron (001) surfaces were chosen with 15  $\text{\AA}$  vacuum in order to avoid interactions with its periodic images, and the slab thicknesses of  $\alpha$ - $B_{12}$  and  $\gamma$ - $B_{28}$  are 8.012  $\text{\AA}$  and 6.914  $\text{\AA}$ , respectively. The fully relaxed  $\alpha$ - $B_{12}$  (001) surface with cell vectors is shown in Fig. 1. Here we need to point out that the (001) surface of the current study is in a rhombohedral setting and the (001) surfaces of earlier studies [26,31,38] are in hexagonal settings. The Brillouin zone was sampled by  $6 \times 6 \times 1$  k-points using the Monkhorst–Pack scheme. The calculations of  $N_2$  and  $CH_4$  adsorption on  $\alpha$ - $B_{12}$  (001) and  $\gamma$ - $B_{28}$  (001) surfaces are based on the fully optimized surfaces. We have considered all the possible adsorption sites for  $N_2$  and  $CH_4$  adsorption on  $\alpha$ - $B_{12}$  and  $\gamma$ - $B_{28}$  surfaces. What we discussed in the manuscript is the most stable adsorption site. The transition state between chemisorption and physisorption of  $N_2$  was investigated using the complete LST (linear synchronous transit)/QST (quadratic synchronous transit) method [39] implemented in Dmol3 code.

The adsorption energy of  $N_2$  and  $CH_4$  on  $B_{12}$  cluster,  $\alpha$ - $B_{12}$  and  $\gamma$ - $B_{28}$  surfaces are calculated from the following equation:

$$E_{ads} = (E_B + E_{gas}) - E_{B-gas} \quad (1)$$

where  $E_{B-gas}$  is the total energy of boron adsorbent with adsorbed gas,  $E_B$  is the energy of isolated boron adsorbent, and  $E_{gas}$  is the energy of isolated gas molecule, such as  $N_2$  and  $CH_4$ . Electron

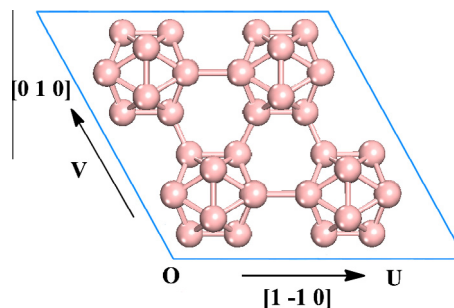


Fig. 1. The fully relaxed  $\alpha$ - $B_{12}$  (001) surface with cell vectors and the surface is in a rhombohedral setting. Atom color code: pink, boron. (For interpretation of the references to color in this figure legend, the reader is referred to the web version of this article.)

Download English Version:

<https://daneshyari.com/en/article/6641479>

Download Persian Version:

<https://daneshyari.com/article/6641479>

[Daneshyari.com](https://daneshyari.com)